10. Slack BE, Richardson U, Nitsch RM, Wurtman RJ. Dioctanoylglycerol stimulates accumulation of [methyl-^{14}C]choline and its incorporation into acetylcholine and phosphatidylcholine in a human cholinergic neuroblastoma cell line. *Brain Res* 1992;585:169–176.
11. Pardridge WM. Transport of nutrients and hormones through the blood-brain barrier. *Fed Proc* 1984;43:201–204.
12. Alger JR, Frank JA, Bizzi A, et al. Metabolism of human gliomas: assessment with H-1 MR spectroscopy and F-18 fluorodeoxyglucose PET. *Radiology* 1990;177:633–641.
13. Fulham MJ, Bizzi A, Dietz MJ, et al. Mapping of brain tumor metabolites with proton MR spectroscopic imaging: clinical relevance. *Radiology* 1992;185:675–686.
14. Miller BL. A review of chemical issues in ^{1}H NMR spectroscopy: N-acetyl-L-aspartate, creatine and choline. *NMR Biomed* 1991;4:47–52.
15. Comar D, Cartron JC, Maziere M, Marazano C. Labeling and metabolism of methionine-methyl-^{11}C. *Eur J Nucl Med* 1976;1:11–14.
16. Fox PT, Mintun MA. Noninvasive functional brain mapping by change-distribution analysis of averaged PET images of $H_2{}^{15}O$ tissue activity. *J Nucl Med* 1989;30:141–149.
17. Coleman RE, Hoffman JM, Hanson MW, Sostman HD, Schold SC. Clinical application of PET for the evaluation of brain tumors. *J Nucl Med* 1991;32:616–622.
18. Janus TJ, Kim EE, Tilbury R, Bruner JM, Yung WKF. Use of [^{18}F]fluorodeoxyglucose positron emission tomography in patients with primary malignant brain tumors. *Ann Neurol* 1993;33:540–548.
19. Glantz MJ, Hoffman JM, Coleman RE, et al. Identification of early recurrence of primary central nervous system tumors by [^{18}F]fluorodeoxyglucose positron emission tomography. *Ann Neurol* 1991;29:347–355.
20. Derlon JM, Bourdet C, Bustany P, et al. [^{11}C]L-Methionine uptake in gliomas. *Neurosurgery* 1989;25:720–728.
21. Ogawa T, Kanno I, Shishido F, et al. Clinical value of PET with ^{18}F-fluorodeoxyglucose and L-methyl-^{11}C-methionine for diagnosis of recurrent brain tumor and radiation injury. *Acta Radiol* 1991;32:197–202.
22. Ogawa T, Hatazawa J, Inugami A, et al. Carbon-11-methionine PET evaluation of intracerebral hematoma: distinguishing neoplastic from non-neoplastic hematoma. *J Nucl Med* 1995;36:2175–2179.
23. Barrio JR. Biochemical principles in radiopharmaceutical design and utilization. In: Phelps ME, Mazziotta JC, Schelbert HR, eds. *Positron emission tomography and autoradiography: principles and applications for the brain and heart.* New York: Raven Press; 1986:451–492.
24. Maziere C, Maziere JC, Mora L, Polonovski J. Early increase in phosphatidylcholine synthesis by choline and transmethylation pathways in spreading fibroblasts. *Exp Cell Res* 1986;167:257–261.
25. Lakher MB, Wurtman RJ. Molecular composition of the phosphatidylcholines produced by the phospholipid methylation pathway in rat brain in vivo. *Biochem J* 1987;244:325–330.
26. Ishiwata K, Kubota K, Murakami M, et al. Re-evaluation of amino acid PET studies: can the protein synthesis rates in brain and tumor tissues be measured in vivo? *J Nucl Med* 1993;34:1936–1943.
27. Ishiwata K, Enomoto K, Sasaki T, et al. A feasibility study on L-[1-carbon-11]tyrosine and L-[methyl-carbon-11]methionine to assess liver protein synthesis by PET. *J Nucl Med* 1996;37:279–285.
28. Eng J, Berkowitz BA, Balaban RS. Renal distribution and metabolism of [$^{2}H_9$]choline. A ^{2}H NMR and MRI study. *NMR Biomed* 1990;3:173–177.
29. Grossman EB, Hebert SC. Renal inner medullary choline dehydrogenase activity: characterization and modulation. *Am J Physiol* 1989;256:107–112.
30. Zeisel SH, Story DL, Wurtman RJ, Brunengraber H. Uptake of free choline by isolated perfused rat liver. *Proc Natl Acad Sci USA* 1980;77:4417–4419.
31. Pritchard PH, Vance DE. Choline metabolism and phosphatidylcholine biosynthesis in cultured rat hepatocytes. *Biochem J* 1981;196:261–267.
32. Pelech SL, Pritchard PH, Vance DE. Prolonged effects of cyclic AMP analogs on phosphatidylcholine biosynthesis in cultured rat hepatocytes. *Biochem Biophys Acta* 1982;713:260–269.
33. Storch KJ, Wagner DA, Young VR. Methionine kinetics in adult men: effect of dietary betaine on L-[$^{2}H_3$-methyl-1-^{13}C]methionine. *Am J Clin Nutr* 1991;54:386–394.
34. Svane-Knudsen V, Rasmussen G, Clausen PP. Surfactant-like lamellar bodies in the mucosa of the human nose. *Acta Otolaryngol* 1990;109:307–313.
35. Snyder F, Malone B. Acyltransferases and the biosynthesis of pulmonary surfactant lipid in adenoma alveolar type II cells. *Biochem Biophy Res Commun* 1975;66:914–919.
36. Rooney SA. The surfactant system and lung phospholipid biochemistry. *Am Rev Respir Dis* 1985;131:439–460.
37. Arneric SP, Honig MA, Milner TA, Greco S, Iadecola C, Reis DJ. Sites of acetylcholine synthesis and release associated with microvessels in cerebral cortex: ultrastructural and neurochemical studies. *J Cereb Blood Flow Metab* 1987;7:S330.
38. Hamel E, Assumel-Lurdin C, Edvinsson L, Fage D, MacKenzie ET. Neuronal versus endothelial origin of vasoactive acethylcholine in pial vessels. *Brain Res* 1987;420:391–396.
39. Estrada C, Bready J, Berliner J, Cancilla PA. Choline uptake by cerebral capillary endothelial cells in culture. *J Neurochem* 1990;54:1467–1473.
40. Galea E, Estrada C. Ouabaine-sensitive choline transport system in capillaries isolated from bovine brain. *J Neurochem* 1992;59:936–941.
41. Peeling J, Sutherland G. High-resolution ^{1}H NMR spectroscopy studies of extracts of human cerebral neoplasms. *Magn Reson Med* 1992;24:123–136.
42. Usenius JPR, Kauppinen RA, Vainio PA, et al. Quantitative metabolite patterns of human brain tumors: detection by ^{1}H NMR spectroscopy in vivo and in vitro. *J Comput Assist Tomogr* 1994;18:705–713.
43. Kugel H, Heindel W, Ernestus RI, et al. Human brain tumors: spectral patterns detected with localized H-1 MR spectroscopy. *Radiology* 1992;183:701–709.

Comparison of Copper-67- and Iodine-125-Labeled Anti-CEA Monoclonal Antibody Biodistribution in Patients with Colorectal Tumors

Angelika Bischof Delaloye, Bernard Delaloye, Franz Buchegger, Charles-André Vogel, Michel Gillet, Jean-Pierre Mach, Alan Smith and P. August Schubiger

Departments of Nuclear Medicine and Surgery, Institute of Biochemistry, University of Lausanne, Lausanne; and Division of Radiopharmacy, Paul Scherrer Institute, Villigen, Switzerland

Copper-67 has comparable beta-particle emissions to that of ^{131}I, but it displays more favorable gamma emission characteristics for application in radioimmunotherapy (RIT). This study investigates the potential of ^{67}Cu-labeled monoclonal antibody (MAb) 35 for RIT of colorectal carcinoma. **Methods:** Biokinetics of simultaneously injected ^{67}Cu- and ^{125}I-labeled MAb35 were studied in six patients scheduled for surgery of primary colorectal cancer. **Results:** Whole-body clearance ($T_{1/2}$) of ^{67}Cu, estimated from sequential anterior and posterior whole-body scans and corrected for decay of ^{67}Cu, was 41 hr. Serum clearance of ^{67}Cu was faster (27.41 hr) than that of ^{125}I (38.33 hr). Mean tumor uptake of the ^{67}Cu-labeled compound (0.0133 %ID/g) exceeded that of ^{125}I (0.0095 %ID/g), and tumor-to-blood ratios were higher for ^{67}Cu than for ^{125}I, with averages of 6.07 and 2.41, respectively. The average ^{67}Cu/^{125}I ratio was 1.9 for tumor uptake, 0.7 for blood and 2.6 for tumor-to-blood ratios. Nonspecific liver uptake of ^{67}Cu as calculated from whole-body scans was high in four patients, up to 25% of residual whole-body activity at 48 hr, but did not increase with time. We also observed some nonspecific bowel activity, as well as moderate to high uptake in benign polyps. **Conclusion:** Copper-67-labeled MAb35 is more favorable than its radioiodine-labeled counterpart for RIT of colorectal carcinoma due to higher tumor-to-blood ratios, but the problem of nonspecific liver and bowel uptake must first be overcome. The absolute accumulation of activity in tumor remains low, however, so the probability of cure with this compound alone is questionable. The use of ^{67}Cu as one component of a multimodality adjuvant treatment seems to remain the most appropriate application for RIT.

Key Words: anti-CEA; monoclonal antibodies; radioimmunotherapy; copper-67; iodine-125; colorectal carcinoma

J Nucl Med 1997; 38:847–853

Received May 13, 1996; revision accepted Nov. 6, 1996.

For correspondence or reprints contact: Angelika Bischof Delaloye, MD, Nuclear Medicine Department, Centre Hospitalier Universitaire Vaudois, CH-1011 Lausanne, Switzerland.

Most radioimmunotherapy (RIT) trials have been performed with ^{131}I-labeled monoclonal antibodies (MAb) (*1–11*). Despite advantages such as low price, extensive experience with ^{131}I in

the treatment of thyroid diseases and low incidence of major side effects with therapeutic doses currently used, this radionuclide is far from being ideal for RIT. The high-energy gamma emission of ^{131}I (364 keV, 82%) accounts for two-thirds of the absorbed dose equivalent of this nuclide (*12*) and thus contributes substantially to the radiation burden of the patient. In particular, the unwanted dose to the bone marrow, which is the dose-limiting factor in RIT, is unnecessarily accentuated by the gamma emission of ^{131}I. Due to the high-energy gamma emission, patients have to be treated in specially equipped rooms, where they are isolated for slightly longer periods than is necessary for the treatment of thyroid malignancies. The need for hospitalization might diminish the acceptance of this treatment by patients, and it increases the cost of the procedure. The relatively high-radiation exposure of the nursing staff is also to be taken into consideration. Furthermore, residence time of radioiodine at the target tumor is reduced by dehalogenation (*13*). The modest tumor dose in comparison with a relatively high exposure of the bone marrow is not in favor of a widespread use of ^{131}I-labeled MAb as an adjuvant treatment of frequent solid tumors, such as colorectal carcinoma, and minimal residual disease seems to be the most promising target for RIT. Bone marrow transplantation might certainly overcome bone marrow depression, but this procedure appears impractical as part of an adjuvant treatment setting on a routine base.

Copper-67 has been proposed as an interesting alternative to ^{131}I for application in RIT (*14–16*). Its main gamma emission is less abundant and energetic (185 keV, 42%) than that of ^{131}I and is thus convenient for biokinetic measurements and tumor detection by gamma camera, while reducing the radiation burden to patients and staff. The physical half-life of ^{67}Cu, 61 hr, compared to 193 hr for ^{131}I, is also more suitable for application with contemporary vehicles used for RIT. The maximum energy of the beta emission of ^{67}Cu is 0.57 MeV and is thus very close to that of ^{131}I at 0.61 MeV. The maximum range of beta radiation of ^{67}Cu in tissue is 2.2 mm, which is suitable for irradiation of small tumor deposits. Previous experience with animals has shown relatively high tumor uptake and retention of ^{67}Cu-labeled anticolon carcinoma MAb35 when compared to its radioiodine-labeled counterpart (*17*). These results have been supported by studies with MAbs against other solid tumors (*18*) and against tumors of lymphatic origin (*19*), the latter results being confirmed in preliminary clinical studies in patients with lymphoma (*20*). These results encouraged us to study the biodistribution of the ^{67}Cu-labeled anti-carcinoembryonic antigen (CEA) antibody MAb35 in patients with colorectal cancer in the hope of confirming preclinical observations and determining the suitability of this conjugate for RIT.

MATERIALS AND METHODS

Radioimmunoconjugate

MAb35, a murine antibody directed against CEA that has been used successfully in imaging of colorectal tumors after labeling with ^{123}I (*21,22*), was generated commercially as ascites. Purification was performed by protein A chromatography. Purity and molecular weight of the product were assessed by nonreducing sodium dodecyl sulfate-polyacrylamide gel electrophoresis, and then the antibody was transferred by dialysis into a storage buffer (0.1 *M* Tris/0.15 *M* NaCl, pH 7.3) before it was frozen at −80°C.

Copper-67 was produced at the Paul Scherrer Institute, Villigen, Switzerland, as previously described (*23*).

The 14N4 ligand was prepared as originally described (*24*), and its purity assessed by NMR and infrared spectrometry. In total, 3.1 mg of 14N4, 7.6 mg of *N*-(3-dimethylaminopropyl)-*N'*-ethylcarbodiimide and 1.6 mg of *N*-hydroxysulfosuccinimide sodium salt were added to 0.11 ml of 0.1 *M* sodium phosphate, pH 7.0, and then the reaction volume was increased to 0.22 ml with the same buffer. The reaction mix was stirred for 1 hr at room temperature, and then the pH was adjusted back to 7.0 with 1 *M* NaOH. A 187.5-μl aliquot of this mixture was added to 12 mg of intact MAb35 in 1.0 ml of 0.1 *M* phosphate buffer, pH 7.0. After 1 hr of stirring at ambient temperature, the ligand-substituted MAb35 was purified on a fast protein liquid chromatography column pre-equilibrated with 0.2 *M* succinate buffer, pH 4.0, and eluted in the same buffer ready for labeling.

For labeling of 14N4-conjugated MAb, 5 mCi (185 MBq) of ^{67}Cu (Paul Scherrer Institute) was taken up in 500 μl of 0.2 *M* succinate buffer, pH 4.0, and then added to 10 mg of MAb35 in the same buffer. The mixture was stirred for 30 min at ambient temperature, and then 50 μl of saturated 14N4 solution was added to chelate nonincorporated copper. After 5 min, the whole reaction mixture was loaded onto a fast protein liquid chromatography column, pre-equilibrated with phosphate-buffered saline, pH 7.4, and eluted in the same buffer. The number of 14N4 ligands per antibody molecule has been previously calculated at the molar ratios of 64:1, chelator-to-antibody. Each antibody molecule has, on average, 4.5 chelator molecules (*25*). Nonconjugated MAb35 was labeled with ^{125}I by the Iodo gen technique. The labeled antibody was sterile-filtered and subjected to a standard protocol of quality control testing, including sterility, pyrogenicity, osmolality, pH, radiochemical purity and free radionuclide determination.

Immunoreactivity of both preparations was determined in a direct binding assay on CEA insolubilized on CNBr-Sepharose. Serum samples of patients obtained during the first hour after injection were also incubated with packed CEA-Sepharose. Nonspecific binding was measured by incubation with irrelevant protein, also coupled to CNBr-Sepharose and subtracted from CEA-binding values as previously described (*26*).

Specific activity was 0.1–0.5 mCi/mg (3.7–18.5 MBq/mg) MAb for ^{67}Cu and 0.8–1.2 mCi/mg (29.6–44.4 MBq/mg) MAb for ^{125}I. The same protein dose was injected in all patients: 10 mg of MAb labeled with ^{67}Cu and 0.2 mg of MAb labeled with ^{125}I. At the moment of injection, immunoreactivity was 86% ± 4% for the ^{67}Cu-labeled compound and 86% ± 5% for the ^{125}I-labeled one. Nonspecific binding of both conjugates was less than 1.5%. At the calibration point, 6 hr after antibody labeling, the ^{67}Cu/^{64}Cu ratio was at worst 0.7; however, due to the rapid half-life of ^{64}Cu in comparison to ^{67}Cu (12.7 hr and 61.9 hr, respectively), at the time of patient administration, this ratio had increased to approximately 4.1. A 25% contamination by ^{67}Cu causes less than 10% deviation in activity quantification of ^{67}Cu (*27*). This impurity was not considered problematic in the present imaging study. Mean injected activity was 4.43 (range, 1.29–8.78) mCi (164 MBq; range, 48–325 MBq) for ^{67}Cu and 0.1 (range, 0.07–0.2) mCi (3.7 MBq; range, 2.6–7.4 MBq) for ^{125}I.

Patients

Six patients (five men and one woman) scheduled for resection of a primary tumor of the colon (n = 4) or rectum (n = 2) were included after having given informed consent (Table 1). Mean age was 69 yr (range, 47–86). According to a routine protocol accepted by the Institutional Review Board, patients were premedicated with an antihistaminic drug (Clemastine, 2 mg) and had the thyroid blocked by the administration of potassium iodide (100 mg b.i.d. starting the day of injection and continued until surgery). A blood sample for the determination of serum CEA and human anti-mouse antibodies was drawn before infusion.

Both labeled compounds were diluted in 100 ml of normal saline and simultaneously infused via an intravenous catheter over 30 min. Subsequently, blood samples were obtained at various time

TABLE 1
Patient Data

Patient no.	Sex	Age (yr)	CEA (ng/ml)	Tumor site	Size estimate (cm^3)	Stage			Operation (dpi)
						Dukes	Jass	TNM	
1	M	76	3.1	Splenic angle	6	B	II	T3N0Mx	6
2	M	47	4.2	Splenic angle	84	C	II	T3N1Mx	8
3	M	62	1.3	Cecum	33	C	IV	T3N2Mx	5
4	M	86	1110	Cecum	60	C	IV	T3N3M1	6
5	F	66	21.7	Rectum	11	B	II	T3N0Mx	6
6	M	77	0.5	Rectum	9	A	I	T1N0Mx	2

dpi = days postinjection; TNM = tumor-node metastasis.

points. Simultaneous anterior and posterior whole-body scans were performed 1 hr as well as 1 and 2 days after injection. Planar views and SPECT of the body region where the tumor was located were included when the patient's condition allowed.

Serum activity was counted on both photopeaks, corrected for spillover and expressed in percent of the activity of the first sample taken immediately after the end of infusion. Total-body activity was measured as the geometric mean of the total counts of simultaneously acquired anterior and posterior whole-body scans. Liver uptake (geometric mean of anterior and posterior liver counts) was estimated in percent of whole-body activity. No correction was made for residual ^{64}Cu activity. Surgery was performed 2–8 days after injection, and samples of tumor, normal colonic mucosa, fat and blood were counted in all patients. In two patients (Patients 1 and 4), activity of benign polyps was also measured, as well as that of a metastatic lymph node in Patient 4. All blood and tissue samples were counted on both photopeaks, corrected for spillover and weight, and results were expressed as percent injected dose (%ID)/g.

RESULTS

Injection of the two conjugates was well tolerated; none of the patients showed any adverse reaction and none had preexisting human anti-mouse antibodies. Immunoreactivity of the labeled conjugates was determined in the first serum samples after injection, it was 82% ± 6% and 82% ± 5% for the ^{67}Cu- and ^{125}I-labeled MAb, respectively, with nonspecific binding being less than 1.5% for both.

The ^{67}Cu-labeled MAb35 demonstrated tumor accumulation on whole-body scintigraphy in all but two patients. In one of them (Patient 2), the injected activity was very low and the tumor could be faintly distinguished only on emission computerized tomography. In the other patient (Patient 1), activity in a benign polyp was taken for the primary tumor. In fact, the activity of the polyp was greater than that of the tumor. In another patient, there was also uptake in a benign polyp, but in this case the uptake was clearly less pronounced than in the tumor.

Except for Patients 1 and 6, liver activity was rather high at all time points (Fig. 1), with up to 11% of whole-body activity at 1 hr and up to 16% and 25% of residual whole-body activity at 24 and 48 hr, respectively. Absolute liver activity, in percent of initial whole-body activity, remained rather stable during the 48-hr observation period. The level of liver accumulation of the ^{67}Cu-labeled MAb35 did not correlate strictly with increased serum CEA. In Patient 4, whose serum CEA level was very high (1110 ng/ml) and in whom previously unsuspected liver metastases were detected during subsequent surgery, liver uptake in percent of residual whole-body activity was comparable to that of Patients 3 and 5, whose serum levels of CEA were 1.3 and 21.7 ng/ml, respectively.

There was also some uptake in the large bowel in three patients (Fig. 1) that exceeded what we observe when using the same MAb labeled with ^{123}I.

No prominent kidney uptake was observed. In one patient, urinary activity could be measured at 17, 23 and 40 hr after injection. Urinary elimination of iodine was slightly higher (2.8,

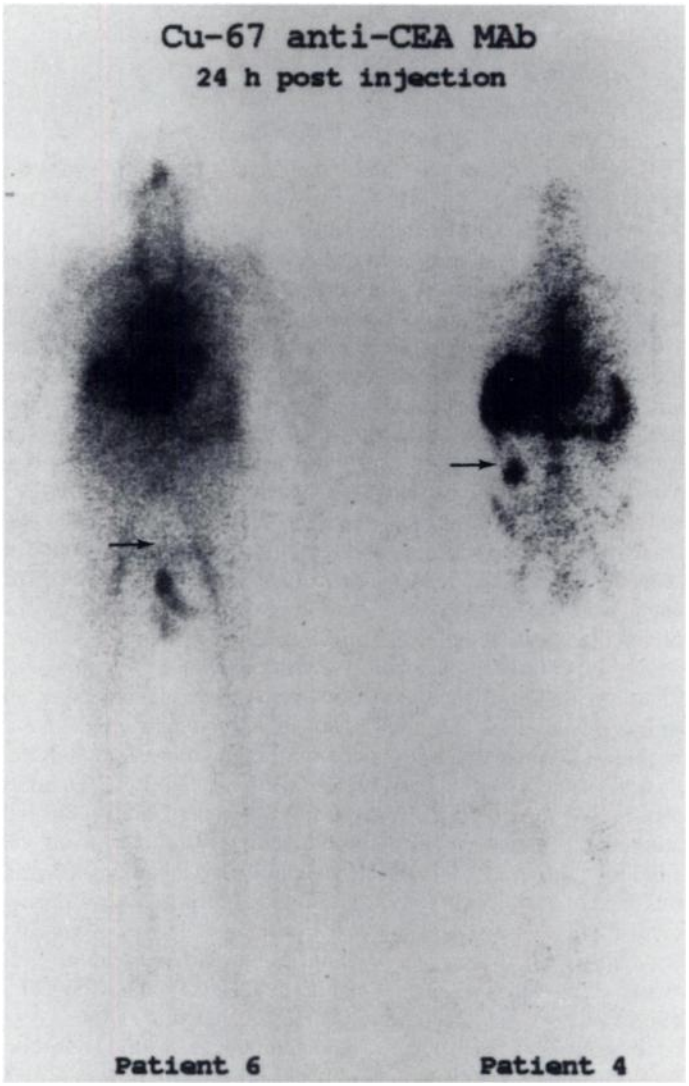

FIGURE 1. Anterior whole-body scans of two patients 24 hr after injection of ^{67}Cu-labeled MAb35. In Patient 6 (left), the tumor of the rectum (arrow) is only faintly visible on the anterior scan, whereas the carcinoma of the cecum/ascending colon (right, arrow) of Patient 4 is clearly shown. The scans show the difference of liver and bone marrow uptake in these two patients. Serum CEA was 0.5 ng/ml in Patient 6 and 1110 ng/ml in Patient 4, in whom liver metastases were discovered at surgery.

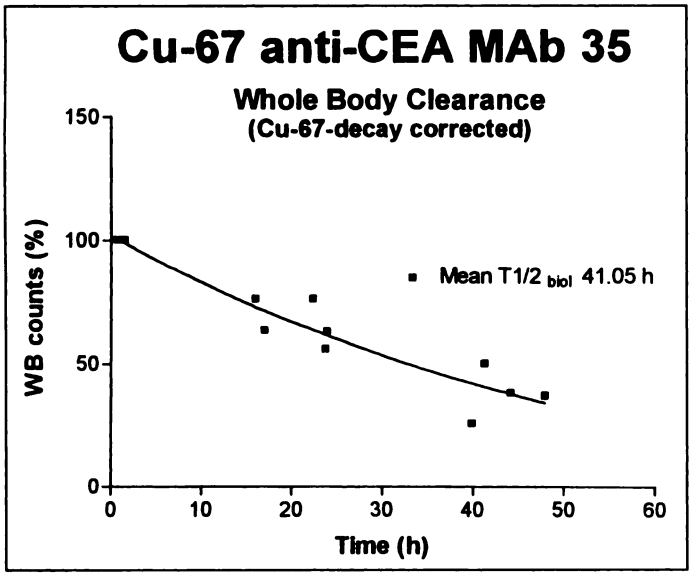

FIGURE 2. Whole-body clearance of ^{67}Cu-labeled MAb35, derived from the early decay-corrected geometric mean of sequential anterior and posterior whole-body scans.

2.2 and 8.9 %ID/liter, respectively) than that of copper (1.7, 2.6 and 5.0 %ID/liter, respectively), but the ^{67}Cu/^{125}I ratio remained stable (0.6) for all three collections.

Decay-corrected mean whole-body clearance (biological $T_{1/2}$) of ^{67}Cu was 41.05 hr (Fig. 2). Figure 3 shows decay-corrected serum clearance of both radionuclides. Counts were expressed in percent of those of the first sample taken immediately after the end of MAb infusion (time 0), in which the activity corresponded to 0.0244 (range, 0.0179–0.0290) %ID/g for ^{67}Cu and 0.0232 (range, 0.0142–0.0302) %ID/g for ^{125}I. Clearance was biexponential, but the short collection period did not allow reliable separation of the slow and fast components. Mean $T_{1/2}$ was 27.41 hr for ^{67}Cu and 38.33 hr for ^{125}I. The faster disappearance of ^{67}Cu was confirmed by the lower blood activity of this radionuclide in the preoperative samples. Mean blood activity of ^{67}Cu (Table 2) was 0.0028%ID/g (range, 0.0006–0.0082) and that of ^{125}I (Table 3) 0.004%ID/g (range, 0.0012–0.0105). With a mean tumor uptake of 0.0133%ID/g (range, 0.0036–0.0235) for ^{67}Cu and 0.0095%ID/g (range, 0.0025–0.0205) for ^{125}I, a more favorable tumor-to-blood ratio was obtained for the former (on average, 6.07 and 2.41, respectively). The two polyps showed high uptake of ^{67}Cu. Presence of CEA in the polyps was confirmed by immunoperoxidase staining. Uptake was particularly prominent in the polyp of Patient 1, which contained foci of marked dysplasia and where tumor uptake was exceeded (0.0492 versus 0.0176 %ID/g) 6 days after administration of the labeled antibodies. In this patient, except for an overall lower uptake, findings with the ^{125}I-labeled compound were comparable with uptakes of 0.0223 and 0.0094 %ID/g for polyp and tumor, respectively. The tumor-to-polyp ratio was 0.36 for ^{67}Cu and 0.42 for ^{125}I in this patient. In Patient 4, uptake of both radionuclides in a benign polyp with moderate dysplasia, also measured 6 days after injection, was increased, but the uptakes were less than in the first patient, at 0.0101 and 0.0032 %ID/g for ^{67}Cu and ^{125}I, respectively. The tumor-to-polyp ratio in this patient was 1.71 for ^{67}Cu and 1.45 for ^{125}I. In the same patient, we were also able to measure activity of a small metastatic lymph node, which was very favorable for ^{67}Cu (0.0267 %ID/g), whereas no increased uptake of the ^{125}I-labeled compound was observed (0.0017 %ID/g). Metastasis-to-blood ratio was 14.12 for ^{67}Cu and 0.77 for ^{125}I (Table 4).

DISCUSSION

These human data confirm the higher tumor uptake and the more favorable tumor-to-blood ratio for the ^{67}Cu-labeled MAb35 antibody in comparison to the radioiodinated form of the same antibody as observed in the nude mouse model proposed by Smith et al. (*17*). In these preclinical studies, it was found that tumor-to-blood ratios increased steadily for both compounds from Day 1 to Day 7 (^{67}Cu, 1.48–5.6; ^{131}I, 0.98–1.86) but remained much lower for iodine at all time points. Using the same antibody in humans, we found similar differences between the two labels, with the average tumor-to-blood ratio being 6.07 for ^{67}Cu and 2.63 for ^{125}I at a mean interval of 5.5 days after injection. In the single patient who was operated on only 2 days postinjection, the tumor-to-blood ratio was lower for both radionuclides, especially for copper (2.86), whereas the difference was less striking for iodine (1.95). Even at this earlier time point, the ratio was still in favor of the copper-labeled conjugate (Fig. 4). The overall mean tumor-to-blood ratio for ^{67}Cu was 2.63 times higher than that of ^{125}I. Urinary excretion was 1.7 times higher for iodine. The mean ^{67}Cu/^{125}I ratio in the tumors was 1.9 ± 1.04 (±1 s.d.), with a rather large coefficient of variation of 55%. The ratio was 0.70 ± 0.21 (coefficient of variation, 30%) in blood. The variation was mainly due to the fact that the interval between injection and surgery varied among the patients. The difference of the interval between labeling with ^{67}Cu and injection and, as a consequence, the difference of contamination by ^{64}Cu were probably less significant. According to the data of Shen et al. (*27*), a 25% contamination of the ^{67}Cu compound with ^{64}Cu introduces a 10% deviation in activity counting. Whole-body scintigraphy being a relatively crude method for quantifying activity distribution, we did not consider this additional uncertainty problematic.

All blood and tissue samples were counted after complete decrease of ^{64}Cu to obtain reliable data on the biokinetics of ^{67}Cu-labeled MAb35 and of the simultaneously injected ^{125}I-labeled MAb35. Our data suggest at least prolonged retention of ^{67}Cu in the tumor, if not an increased in vivo stability of the ^{67}Cu-labeled conjugate, whereas the iodine-labeled form is susceptible to dehalogenation. Due to the longer tumor residence time for ^{67}Cu, a more favorable therapeutic ratio can be expected. The faster blood clearance of the ^{67}Cu-labeled MAb is in contradiction with observations of DeNardo et al. (*20*), who found no significant difference in the clearance of ^{131}I- and ^{67}Cu-labeled Lym-1 MAb, which is directed against malignant B cells. They also observed high tumor uptake of the ^{67}Cu-labeled compound together with a relatively high liver uptake, but no accumulation in normal bone marrow. In our patients, faint bone marrow uptake was seen in some cases, but it was not striking enough to allow any attempt of quantification from the imaging studies. The most prominent uptake of bone marrow was observed in the patient with liver metastases and a particularly high circulating CEA level (1110 ng/ml). One may speculate that this particular finding is due to the presence of immune complexes (*26*), but we have not performed analytical size chromatography on the sera to confirm this hypothesis. Liver uptake of ^{67}Cu was much higher than described in animal models with copper-labeled MAb35, Lym-1 and 1A3 antibodies (*17,20,28*). This latter antibody, which binds to a lipid antigen enriched in human colon carcinoma cells, has been used after being labeled with ^{64}Cu in patients with colorectal adenocarcinomas. It allowed successful PET imaging of the primary tumors but, as in our study with ^{67}Cu, relatively high liver uptake was observed in humans and prevented detection of three of five liver metastases in this small series (*29*).

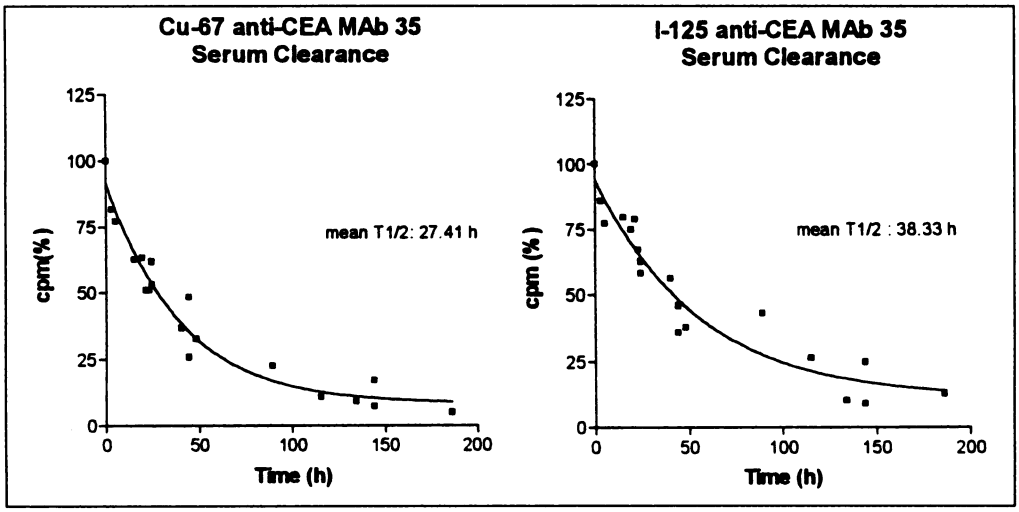

FIGURE 3. Serum clearance of ^{67}Cu- (left) and ^{125}I- (right) labeled MAb35. The activity is expressed for each patient as percent of the activity per ml of the first sample taken at the end of antibody infusion. In this sample, mean activity in %ID/g was 0.0244 (range, 0.0179–0.0290) for ^{67}Cu and 0.02322 (range, 0.0142–0.0302) for ^{125}I. The mean $T_{1/2}$ is faster for the ^{67}Cu-labeled compound (27.41 hr) than for the ^{125}I-labeled conjugate (38.33 hr).

Uptake in bone marrow was discrete and should not represent a dose-limiting factor for RIT, in which it can be overcome by bone marrow rescue or administration of hematopoietic growth factors. The high liver uptake, however, must be taken into consideration when planning the use of the ^{67}Cu-labeled MAb35 in an adjuvant therapy setting in patients with colorectal carcinoma. Administration of free chelator may be useful in decreasing the copper content of liver cells (*30*). The use of $F(ab')_2$ or even smaller fragments would probably also decrease the liver uptake but at the expense of an increased kidney accumulation. The activity delivered to the tumor when MAb fragments are used is not necessarily as high as that when intact antibody is used, and tumor residence time would probably decrease (*17*). New labeling procedures, including two- or three-step labeling techniques, might help to decrease nonspecific uptake in normal tissues (*31*), be it in the liver or bone marrow. Bowel cleaning might diminish intraluminal activity and thus the exposure of normal bowel mucosa; no such procedures were ever performed in these patients. Counting of tissue samples has shown, however, that ^{67}Cu uptake in normal mucosa was in the mean two times that of ^{125}I. As assessed by visual inspection, the bowel activity was similar to that observed in patients studied with comparable activities of ^{131}I for the diagnosis of functional metastases of differentiated thyroid carcinomas.

The two polyps showed increased uptake of the immunoconjugate that was certainly related to the presence of CEA as confirmed by immunohistochemistry. None of the polyps showed signs of malignancy, but they did show marked to moderate dysplasia.

The higher tumor uptake, in particular the high activity measured in the single metastatic lymph node studied, the longer tumor residence time and the lower blood background in comparison with the iodine-labeled conjugate are promising for the use of the ^{67}Cu-labeled MAb35 in RIT of small tumor deposits in patients with colorectal carcinoma. Its lower beta energy might be more favorable for the treatment of minimal residual disease than the more energetic beta emitter ^{90}Y (*32*). Accumulation of ^{90}Y in bone may increase dose-limiting toxicity (*33*). Furthermore, the absence of concomitant beta emission does not allow imaging the whole-body distribution of ^{90}Y. O'Donoghue et al. (*34*) have calculated that, for ^{67}Cu, an

TABLE 2
Uptake of Copper-67-Labeled anti-CEA MAb35 in Tumor and Normal Tissues (%ID/g)

Patient no.	Tumor	Miscellaneous	Normal mucosa	Fat	Blood	Tumor-to-blood ratio
1	0.0176	Benign polyp, 0.0492	0.0054	0.0005	0.0027	6.63
2	0.0038		0.0014	0.0003	0.0006	6.15
3	0.0173		0.0062	0.0003	0.0021	8.06
4	0.0101	Benign polyp, 0.0059 Node metastasis, 0.0267	0.0068	0.0003	0.0019	5.34
5	0.0078		0.0037	0.0004	0.0011	7.40
6	0.0235		0.0066	0.0007	0.0082	2.86

TABLE 3
Uptake of Iodine-125-Labeled anti-CEA MAb35 in Tumor and Normal Tissues (%ID/g)

Patient no.	Tumor	Miscellaneous	Normal mucosa	Fat	Blood	Tumor-to-blood ratio
1	0.0094	Benign polyp, 0.0223	0.0031	0.0004	0.0031	3.04
2	0.0035		0.0014	0.0002	0.0012	2.79
3	0.0180		0.0056	0.0005	0.0055	3.27
4	0.0032	Benign polyp, 0.0022 Node metastasis, 0.0017	0.0015	0.0002	0.0022	1.44
5	0.0025		0.0013	0.0002	0.0013	1.98
6	0.0205		0.0059	0.0008	0.0105	1.95

TABLE 4
Copper-67/Iodine-125 Ratio in Tumor and Normal Tissues (%ID/g × 10^3)

Patient no.	Tumor	Miscellaneous	Normal mucosa	Fat	Blood	Tumor-to-blood ratio
1	1.86	Benign polyp, 2.20	1.73	1.27	0.85	2.18
2	1.08		0.99	2.00	0.49	2.20
3	0.96		1.10	0.65	0.39	2.46
4	3.20	Benign polyp, 2.64 Node metastasis, 15.96	4.45	1.67	0.86	3.70
5	3.15		2.72	2.44	0.84	3.74
6	1.14		1.16	0.92	0.78	1.47
Mean	1.90		2.02	1.49	0.70	2.63
s.d.	1.04		1.35	0.67	0.21	0.91
CV	0.55		0.67	0.45	0.30	0.35

s.d. = standard deviation; CV = coefficient of variation.

initial activity of 10.1 MBq, with 3.24 × 10^{12} bound radionuclide atoms per g of tumor, is needed to produce a cure probability of 0.9 at the optimal diameter of 2.0 mm. In the single patient of this series who was operated on only 2 days after injection, tumor uptake was 0.0235 %ID/g. An activity of 42.55 GBq (1150 mCi) would thus be required to fulfill the condition of 10 MBq/g. Besides such theoretical considerations, the final therapeutic effect is also determined by the biological characteristics of each tumor. It is well known that, despite low calculated internal dosimetry values, some therapeutic effects have been obtained with radiolabeled antibodies, especially in lymphomas but exceptionally also in solid tumors.

Copper-67-labeled anti-CEA antibodies, possibly combined with the same or other antibodies labeled with a long-range beta-emitter, may be considered as a potentially useful component of multimodality adjuvant treatment in patients with colorectal carcinoma at high risk of recurrence, in whom long-term prognosis still remains rather poor (*35*).

ACKNOWLEDGMENTS

This work was partly supported by the Swiss Foundation for Scientific Research (grant 31-31238-91); Recherche Suisse contre le Cancer (grant Akt 312); the Schweizerische Krebsliga (grant FOR.267.92); and the Gertrud Hagmann Stiftung, Lommiswil.

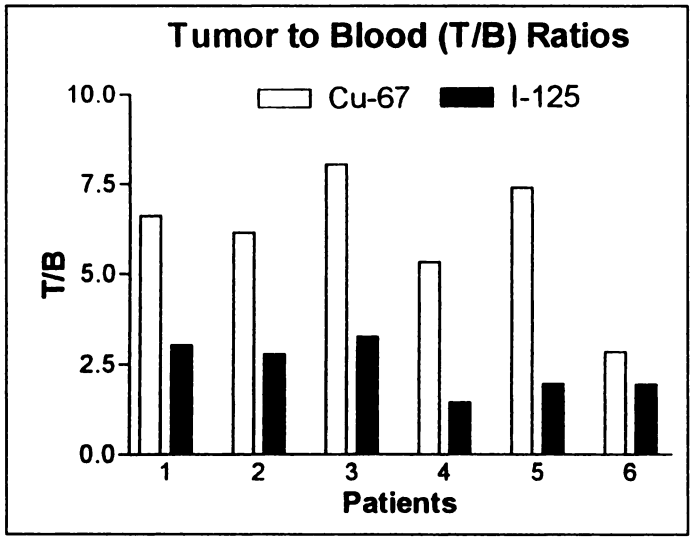

FIGURE 4. Tumor-to-blood ratios for the ^{67}Cu- and ^{125}I-labeled anti-CEA antibody MAb35 measured on surgical specimen obtained in the first five patients between 5 and 8 days and in the last patient 2 days after injection. In all patients, this ratio was in favor of ^{67}Cu. In the patient operated on at 48 hr, however, the difference was less striking.

REFERENCES

1. Carrasquillo JA, Krohn KA, Beaumier P, et al. Diagnosis of and therapy for solid tumors with radiolabeled antibodies and immune fragments. *Cancer Treat Rep* 1984;68:317–328.
2. Delaloye B, Bischof Delaloye A, Pettavel J, et al. Intra-arterial administration of 131-I-anti-CEA-MAb as a therapeutic approach to liver metastases [Abstract]. *Nuklearmedizin* 1987;26:52.
3. Stewart JS, Hird V, Sullivan M, Snook D, Epenetos AA. Intraperitoneal radioimmunotherapy for ovarian cancer. *Br J Obstet Gynecol* 1989;96:529–536.
4. DeNardo GL, DeNardo SJ, O'Grady LF, Levy NB, Adams GP, Mills SL. Fractionated radioimmunotherapy of B-cell malignancies with ^{131}I-Lym-1. *Cancer Res* 1990;50: 1014–1016.
5. Bischof Delaloye A, Delaloye B. Radioimmunotherapy. In: Munz DL, Emrich D, eds. *Immunoscintigraphy. Facts and fiction.* Amsterdam: Excerpta Medica; 1990.
6. Meredith RF, Khazaeli MB, Liu T, et al. Dose fractionation of radiolabeled antibodies in patients with metastatic colon cancer. *J Nucl Med* 1992;33:1648–1653.
7. Kaminski MS, Zasadny KR, Francis IR, et al. Radioimmunotherapy of B-cell lymphoma with [^{131}I]anti-B1 (anti-CD20) antibody. *N Engl J Med* 1993;329:459–465.
8. Press OW, Eary JF, Appelbaum FR, et al. Radiolabeled-antibody therapy of B-cell lymphoma with autologous bone marrow support. *N Engl J Med* 1993;329:1219–1224.
9. Czuczman MS, Strauss DJ, Divgi CR, et al. Phase I dose-escalation trial of iodine 131-labeled monoclonal antibody OKB7 in patients with non-Hodgkin's lymphoma. *J Clin Oncol* 1993;11:2021–2029.
10. Murray JL, Macey DJ, Kasi LP, et al. Phase II radioimmunotherapy trial with ^{131}I-CC49 in colorectal cancer. *Cancer* 1994;73(suppl):1057–1066.
11. Welt S, Divgi CR, Kemeny N, et al. Phase I/II study of iodine 131-labeled monoclonal antibody A33 in patients with advanced colon cancer. *J Clin Oncol* 1994;12:1561–1571.
12. Humm JL. Dosimetric aspects of radiolabeled antibodies for tumor therapy. *J Nucl Med* 1986;27:1490–1497.
13. Andrew SM, Perkins AC, Pimm MV, Baldwin RW. A comparison of iodine and indium labeled anti-CEA intact antibody, F(ab'$_2$) and Fab fragments by imaging tumour xenografts. *Eur J Nucl Med* 1988;13:598–604.
14. Reilly RM. Radioimmunotherapy of malignancies. *Clin Pharm* 1991;10:359–375.
15. Moi MK, Meares CF, McCall MJ, Cole WC, DeNardo SJ. Copper chelates as probes of biological systems: stable copper complexes with a macrocyclic bifunctional chelating agent. *Anal Biochem* 1985;148:249–253.
16. Kukis DL, Diril H, Greiner DP, et al. A comparative study of copper-67 radiolabeling and kinetic stabilities of antibody–macrocycle chelate conjugates. *Cancer* 1994;73: 779–786.
17. Smith A, Alberto R, Blaeuenstein P, Novak-Hofer I, Maecke HR, Schubiger PA. Preclinical evaluation of ^{67}Cu-labeled intact and fragmented anti-colon carcinoma monoclonal antibody MAb35. *Cancer Res* 1993;53:5727–5733.
18. Smith A, Zangemeister-Wittke U, Waibel R, Schenker T, Schubiger PA, Stahel RA. A comparison of ^{67}Cu- and ^{131}I-labeled forms of monoclonal antibodies SEN7 and SWA20 directed against small-cell lung cancer. *Int J Cancer* 1994;8(suppl):43–48.
19. Deshpande SV, DeNardo SJ, Meares CF, et al. Copper-67-labeled monoclonal antibody Lym-1, a potential radiopharmaceutical for cancer therapy: labeling and biodistribution in RAJI tumored mice. *J Nucl Med* 1988;29:217–225.
20. DeNardo G, DeNardo S, Kukis D, Diril H, Suey C, Meares C. Strategies for enhancement of radioimmunotherapy. *Nucl Med Biol* 1991;18:633–640.
21. Delaloye B, Bischof Delaloye A, Buchegger F, et al. Detection of colorectal carcinoma by emission-computerized tomography after injection of ^{123}I-labeled Fab or F(ab')$_2$ fragments from monoclonal anti-carcinoembryonic antigen antibodies. *J Clin Invest* 1986;77:302–311.
22. Bischof Delaloye A, Delaloye B, Buchegger F, et al. Clinical value of immunoscintigraphy in colorectal carcinoma patients: a prospective study. *J Nucl Med* 1989;30: 1646–1656.
23. Schwarzbach R, Zimmerman K, Blaeuenstein P, Smith A, Schubiger PA. Development of a simple and selective separation of ^{67}Cu from irradiated zinc for use in antibody labeling: a comparison of methods. *Appl Radiat Isot* 1995;46:329–336.
24. Studer M, and Kaden T. A one-step synthesis of mono-N-substituted azamacrocycles with a carboxylic group in the side chain and their complexes with Cu^{2+} and Ni^{2+}. *Helv Chim Acta* 1986;69:2081–2086.

25. Smith-Jones PM, Fridrich R, Kaden TA, et al. Antibody labeling with Copper-67 using the bifunctional macrocycle 4-[(1,4,8,11-Tetraazacyclotetradec-1-yl)methyl] benzoic acid. *Bioconj Chem* 1991;2:415–421.
26. Buchegger F, Mach JP, Pèlegrin A, et al. Radiolabeled chimeric anti-CEA monoclonal antibody compared with the original mouse monoclonal antibody for surgically treated colorectal carcinoma. *J Nucl Med* 1995;35:420–429.
27. Shen S, DeNardo GL, DeNardo SJ, et al. Dosimetric evaluation of copper-64 in copper-67–2IT-BAT-Lym-1 for radioimmunotherapy. *J Nucl Med* 1996;37:146–149.
28. Anderson CJ, Connett JM, Schwarz SW, et al. Copper-64-labeled antibodies for PET imaging. *J Nucl Med* 1992;33:1685–1691.
29. Philpott GW, Schwarz SW, Anderson CJ, et al. RadioimmunoPET: Detection of colorectal carcinoma with positron-emitting copper-64-labeled monoclonal antibody. *J Nucl Med* 1995;36:1818–1824.
30. Brewer GJ, Yuzbasiyan-Gurkan V. Wilson disease. *Medicine* 1992;71:139–164.
31. Goodwin DA. Tumor pretargeting [Editorial]. *J Nucl Med* 1995;36:876–879.
32. Howell RW, Rao DV, Sastry KS. Macroscopic dosimetry for radioimmunotherapy: nonuniform activity distribution in solid tumors. *Med Phys* 1989;16:66–74.
33. Langmuir VK. Radioimmunotherapy. Clinical results and dosimetric considerations. *Nucl Med Biol* 1992;19:213–225.
34. O'Donoghue JA, Bardiès M, Wheldon TE. Relationships between tumor size and curability for uniformly targeted therapy with beta-emitting radionuclides. *J Nucl Med* 1995;36:1902–1909.
35. Moertel CG, Fleming TR, Macdonald JS, et al. Fluorouracil plus levamisole as effective adjuvant therapy after resection of stage III colon carcinoma: a final report. *Ann Intern Med* 1995;122:321–326.

Clinical Impact of Somatostatin Receptor Scintigraphy in the Management of Patients with Neuroendocrine Gastroenteropancreatic Tumors

Rachida Lebtahi, Guillaume Cadiot, Laure Sarda, Doumit Daou, Marc Faraggi, Yolande Petegnief, Michel Mignon and Dominique Le Guludec

Departments of Nuclear Medicine, Hôpital Bichat and Gastroenterology, Hôpital Bichat, Paris, France

Somatostatin receptor scintigraphy (SRS) has been used for the detection of gastroenteropancreatic (GEP) tumors. This study evaluates the clinical impact of SRS in GEP tumor detection and its therapeutic implications on patient management. **Methods:** We prospectively studied 160 patients with biologically and/or histologically proven GEP tumors. Before SRS, patients were classified into three groups: gastrointestinal (Group 1; n = 90) patients without known metastases; (Group 2; n = 59) patients with metastases limited to the liver; (Group 3; n = 11) patients with known extrahepatic metastases. The scintigraphic data were compared to the radiological findings. **Results:** In Group 1, without known metastases, conventional imaging detected 53 primary sites in 44 patients: SRS was positive in 68% of these sites and discovered 4 additional primary tumors in 3 patients and 16 metastases in 14 patients. Conventional imaging was negative in 46 patients: SRS discovered 47 new sites in 36 patients. In Group 2, SRS confirmed liver metastases in 95% of patients and discovered 45 new sites in 36 of these patients. In Group 3, SRS disclosed 11 new sites in 7 patients. These results modified patient classification in 38 cases (24%). Surgical therapeutic strategy was changed in 40 patients (25%). **Conclusion:** Somatostatin receptor scintigraphy improves tumor detection, has major clinical significance and should be performed systematically for staging and therapeutic decision making in patients with GEP tumors.

Key Words: somatostatin receptor scintigraphy; gastroenteropancreatic tumors; neuroendocrine tumors

J Nucl Med 1997; 38:853–858

Gastroenteropancreatic (GEP) neuroendocrine tumors are slow-growing tumors, clinically silent for many years and often detected when metastases have developed, most commonly in the liver (*1,2*). Tumor localization is essential since surgery remains the optimal treatment in most patients without metastases (*3–6*). Curative surgery is difficult since primary tumors are frequently very small (<1 cm) and potentially undetectable by conventional imaging. Therefore, patients commonly relapse, suggesting the presence of undetected residual tumors. When liver metastases occur, the staging of these patients is essential for therapeutic management. Additional procedures such as hepatectomy, hepatic artery chemoembolization or even liver transplantation in very selected cases can be proposed in patients with metastases limited to the liver. In case of extrahepatic metastases, chemotherapy and more recently octreotide therapy are most frequently indicated. Tumor localization for accurate staging and therapeutic management justifies the use of new imaging techniques such as endoscopic ultrasonography (EUS) (*7,8*) and somatostatin receptor scintigraphy (SRS) (*9,10*).

SRS has been previously reported as an accurate tool for the detection of neuroendocrine tumors (*11,12*), based on the presence of high-affinity binding sites for somatostatin receptor (*13–16*). The aim of our study was to evaluate prospectively the additional clinical value of SRS and its implication on therapeutic management as compared with conventional imaging in patients with GEP tumors, including EUS, for the investigation of the duodenopancreatic area.

MATERIALS AND METHODS

Patients

The impact of SRS was analyzed in 160 consecutive patients (72 women and 88 men, mean age 52 ± 3 yr) with proven GEP tumors, seen in our institution from November 1992 to September 1995. The study population included 78 patients with Zollinger–Ellison syndrome (ZES), 38 patients with a carcinoid tumor and 44 patients with other types of neuroendocrine tumors. Diagnosis of ZES was based on histopathology and specific biological syndrome (n = 60) or only specific biological syndrome (n = 18). In all of the patients with carcinoid tumors and other neuroendocrine tumors, the diagnosis was histologically confirmed. All together, histological confirmation of tumors was obtained in 142 of 160 patients.

Of the 160 patients, 108 were investigated in the primary staging of GEP tumors. Fifty-two patients were investigated for clinical

Received June 6, 1996; accepted Oct. 15, 1996.
For correspondence or reprints contact: Rachida Lebtahi, Service de Médecine Nucléaire, Hôpital Bichat, 46 rue Henri Huchard, 75018, Paris, France.